



COB-2021-1361

A HYBRID ANALYTICAL-NUMERICAL MODEL FROM THE PROPELLANT TANK UP TO THE THRUSTER OF THE LOW-PRESSURE MICRO-RESISTOJET

Igor Pimentel Guimarães

Daduí Cordeiro Guerrieri

Mechanical Engineering Coordination, CEFET-RJ Campus Itaguaí, Rio de Janeiro, Brazil

igor.guimaraes@aluno.cefet-rj.br, dadui.guerrieri@cefet-rj.br

Abstract. *The increasing number of space missions involving CubeSat demonstrates the importance of those new satellite concept. However, these very small satellites still need to improve their maneuvers capabilities by implementing, for instance, an adequate propulsion system. One interesting propulsion system to be implemented in this class of satellite, in order to enable new mission types, is the Low-Pressure Micro-Resistojet (LPM). Even though there are studies on the thruster part of this propulsion system, there is a lack of studies relating to the fluid behavior through the feed system from the tank up to the thruster. The present work describes the plenum pressure and thrust variation as a function of tank pressure based on the proposed hybrid analytical-numerical model. Numerical results were used to establish a parametric relationship between the tank and the plenum where it was proposed a pressure function with an estimated maximum error of 2.8%. Additionally, the proposed pressure function was combined with the LPM analytical model proposing a new relationship for the thrust equation allowing the use of the tank pressure as a parameter. With this new equation, it is possible to predict pressure behavior through the tank and the plenum, the number of channels, and estimate thrust for different tank pressure. In summary, this hybrid analytical-numerical model helps to design the subsystems of the LPM from the tank up to the thruster, with maximum values of thrust and specific impulse estimated in this article was 0.77 mN and 117.55 s respectively.*

Keywords: *LPM, Nanosatellite, propellant tank, Micro-Thruster, CubeSat*

1. INTRODUCTION

The number of space missions involving nanosatellites has been growing in recent decades. The standardization of these satellites, along with the application of commercial off-the-shelf (COTS) products, has helped to reduce the costs and preparation time of these technologies. This makes access to space much easier, therefore it has been drawing the attention not only from universities, but also commercial organizations and government institutions, which have increasingly been involved with these very small satellites (Pang *et al.*, 2016; Doncaster *et al.*, 2016).

The statistical analysis presented by (Xia *et al.*, 2017) revealed that about 95% of the 357 CubeSats analyzed had an Attitude Determination Control System (ADCS). More than 90% of these actuators presented a magnetic system, and more than a half where reaction-wheel based systems, revealing a predominance of the magnetic ADCS systems over the propulsion systems. The main challenge for these actuator devices is their performance level, many still do not have a high level of pointing accuracy.

A step forward for nanosatellites is the application of an adequate propulsion system, which will allow a more precise orbit control, orbital maneuvers, formation flight, collision avoidance, and orbit transfer. (Quinsac *et al.*, 2020; O'Reilly *et al.*, 2021). A proper propulsion system will enable new types of missions such as large constellation of CubeSats allowing earth observations or even 5G communication (Curzi *et al.*, 2020; Mitra and Agrawal, 2015), interplanetary CubeSat missions (Malphrus *et al.*, 2021), and will also enhance the useful life allowing drag compensation to extend orbit or deorbit the satellite (Jensen and Vinther, 2010).

Due to strict space mission requirements, many nanosatellites are launched without a dedicated propulsion system. Most of the nanosatellites are launched by piggy-back launchers, so, in order to secure the main payload, safety requirements must be tight. Therefore, some propellants such as ammonia, acetone, butane, among others, present relative risks of flammability and health hazards. As opposed to that, water presents no risks, therefore, it is not only considered to be the safest propellant but also presents the best velocity increment

per volume of propellant (Guerrieri *et al.*, 2017).

A promising type of propulsion system is the Low-Pressure Micro-Resistojet (LPM), which can operate with water as a green propellant either in liquid or solid phase. The LPM with ice can achieve low levels of pressure, ranging from 50 Pa up to 600 Pa, in order to operate below the water triple point, meaning that only sublimation is expected to happen. The low level of pressure generates low level of thrust and consequently low level of power consumption. The thrust level varies from 0.1 mN to 2.72 mN, depending on the mission type and power level. Despite the great number of studies on the LPM design, there is still a paucity of experiments and analytical/numerical models regarding the propellant storage tank (Cervone *et al.*, 2015; Guerrieri *et al.*, 2016).

To fulfill this gap of information, previous work done by (Guimarães and Guerrieri, 2020), describes the mass flow rate behavior at the plenum for different boundary conditions of propellant tank and plenum in a CubeSat. The present work aims to describe a model to include the numerical results obtained by (Guimarães and Guerrieri, 2020) with the analytical equations for the plenum and the heater chip of the LPM.

2. LPM CONCEPT

The LPM is a type of electric propulsion, based on Newton's law of motion, which uses electrical power to heat a gas through the heater chip in order to accelerate the propellant and generate thrust. For a LPM based on ice, the propellant is heated at the propellant tank, where the sublimation occurs, then the vapor flows throughout the feed system to the plenum, and finally is expelled through the microchannel of the heater chip, see Figure 1 (Cervone *et al.*, 2015).

Besides Figure 1, the propellant tank can also have the same diameter as the feed system, meaning that only a thin tube would be necessary to store the solid propellant, as proposed by (Guerrieri *et al.*, 2018b). The low pressure and the use of a thin tube as a storage tank helps to avoid sloshing problems, which are very usual with liquid propellants or larger storage tanks (Jensen and Vinther, 2010; O'Reilly *et al.*, 2021). The thruster part, which usually comprehends the plenum and the heater chip, has been the focus of numerous works on this type of propulsion system, therefore the propellant tank and the feed system are areas that need further investigations (Cervone *et al.*, 2015; Guerrieri *et al.*, 2018a).

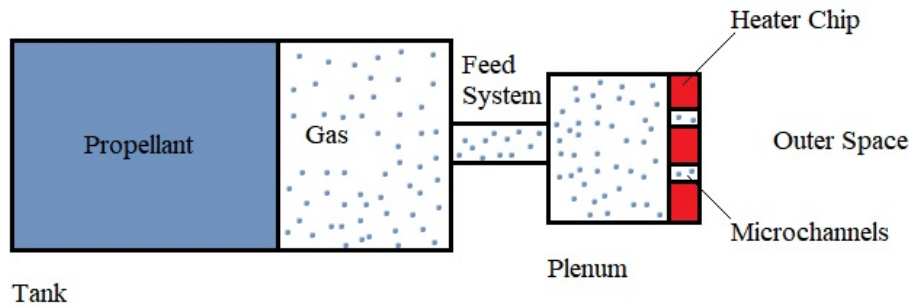


Figure 1. Schematic concept of the LPM (Guimarães and Guerrieri, 2020).

The use of heater chip with a variable number of channels allows for different range of thrust to be achieved. This makes the LPM more flexible in terms of performance, and also the low levels of pressure makes the system more reliable, lighter and less susceptible to leakage problems due to high pressures. The use of a format less complex for the heater chip also benefits its manufacture. Besides nanosatellites like CubeSats, the LPM could match perfectly the mission requirements for classes of picosatellites such as PocketQubes, which demand lower levels of thrust, due to its reduced geometry and mass (Guerrieri *et al.*, 2018b).

The propellant tank of the LPM, when filled with ice, works under sublimation conditions, below the water triple point, making sure that no liquid phase would occur inside the tank. The vapor pressure of water at its triple point is 611 Pa (Guildner *et al.*, 1976). Therefore, the tank is designed to work with a maximum pressure of 600 Pa and a minimum value consistent with the plenum pressure, establishing a pressure gradient among these parts. As proposed by Guimarães and Guerrieri (2020), it is expected a minimum sublimation pressure for the tank is about 300 Pa, which corresponds the maximum pressure for the plenum, and the minimum plenum pressure is 50 Pa.

3. METHODOLOGY

Due to the pressure gradient and the low pressure applied to the LPM, the flow regime varies among each part of the propulsion system, and the Knudsen number Kn is used to identify the flow regime. The Knudsen number is a dimensionless number described by the ratio of the mean free path λ divided by the characteristic length scale D . The continuum regime is represented by $Kn \leq 0.001$; the slip flow regime occurs with $0.001 \leq Kn \leq 0.1$; the transition flow regime happens when $0.1 \leq Kn \leq 10$; and for $Kn \geq 10$ a free-molecular regime is applied (Karniadakis *et al.*, 2006).

The LPM is designed to work on the transitional regime at the plenum to the free-molecular regime in outer space (Silva *et al.*, 2018). Previous studies revealed that for a cylindrical plenum with a 12 mm diameter and a soft tube tank with 0,8 mm of diameter, the slip flow regime is applied throughout the storage tank to the plenum. Guimarães and Guerrieri (2020) performed a numerical simulation to understand the mass flow rate variation throughout the tank to the plenum, considering the pressure limits imposed by the water triple point at the tank and the allowed maximum plenum pressure. Those results are used as input to this work.

Figure 2 presents the mass flow rate as a function of the tank pressure, for different plenum pressure scenarios, based on the numerical simulation data from Guimarães and Guerrieri (2020). Each different line represents a different plenum pressure, and it is noticeable the greater influence of the tank pressure over the mass flow rate, rather than the plenum pressure.

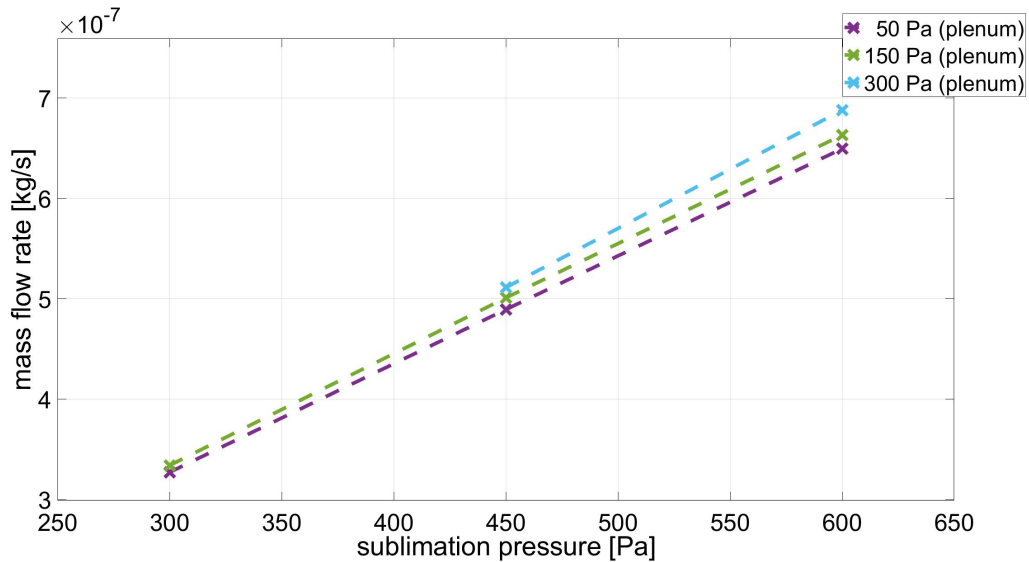


Figure 2. Sublimation pressure versus mass flow rate in the plenum according to Guimarães and Guerrieri (2020).

Assuming that the dispersion of points presented in Figure 2 follows a linear trend, then it is possible to describe it as a first-degree equation as

$$\dot{m} = a \times P_s + b \quad (1)$$

where the coefficients a [$\text{kg s}^{-1} \text{Pa}^{-1}$] and b [kg s^{-1}] are presented in Table 1 according to the respective plenum pressure. Equation (1) represents the variation of the mass flow rate \dot{m} as a function of the sublimation pressure P_s , and it is only valid for a constant plenum pressure described in Table 1, sublimation pressure ranging from 300 Pa to 600 Pa, and a plenum temperature of 300 K.

Table 1. Different coefficients for different plenum pressure

	Plenum pressure		
	50 [Pa]	150 [Pa]	300 [Pa]
a [$\text{kg s}^{-1} \text{Pa}^{-1}$]	1.0746×10^{-9}	1.0969×10^{-9}	1.178×10^{-9}
b [kg s^{-1}]	4.958×10^{-9}	5.5938×10^{-9}	-1.9038×10^{-8}

An analytical model developed by Guerrieri *et al.* (2018a), showed that the mass flow rate, that goes through the channel of the heater chip, can be described as a function of the transmission coefficient α , plenum pressure

P_0 , molecule mass m_a , Boltzmann constant k , plenum temperature T_0 and the exit area A_e . The Equation (2) describes that relation

$$\dot{m} = \alpha P_0 \sqrt{\frac{m_a}{2\pi k T_0}} A_e. \quad (2)$$

It is also commented by the author, that different empirical equations were suggested to describe the transmission coefficient, considering the nature of the channel geometry. For a short uniform circular cross section channel, the transmission coefficient can be described as

$$\alpha = 1 + \delta^2 - \delta \sqrt{\delta^2 + 1} - \frac{[(2 - \delta^2 \sqrt{\delta^2 + 1} + \delta^3 - 2)]^2}{4,5 \delta \sqrt{\delta^2 + 1} - 4,5 \ln(\delta + \sqrt{\delta^2 + 1})} \quad (3)$$

where δ is the channel length to diameter ratio $\delta = \frac{L}{D}$. This equation is only valid for $\delta < 50$.

It is also described by Guerrieri *et al.* (2018a) an analytical model for the thrust of a LPM as

$$\mathfrak{S} = \alpha P_0 A_e \frac{(\pi + 2)}{2\pi} \sqrt{\frac{T_w}{T_0} \left(\frac{6\gamma}{\pi + 6\gamma} \right)}, \quad (4)$$

and the specific impulse as

$$I_{sp} = \frac{(\pi + 2)}{g_0} \sqrt{\frac{k T_w}{2\pi m_a} \left(\frac{6\gamma}{\pi + 6\gamma} \right)} \quad (5)$$

where T_w is the wall temperature of the heater chip, g_0 is the Earth gravitational acceleration at sea level and γ is the specific heat ratio,

Therefore, there is a numerical equation, Eq. (1), that estimates the variation of the plenum mass flow rate as a function of the sublimation pressure, and an analytical Eq. (2) that describes the mass flow rate variation in the heater chip as a function of the plenum pressure. In order to establish a condition of mass conservation throughout the system, the mass flow rate in Eq. (1) can be equated to the mass flow rate in Eq. (2) resulting in the Eq. (6);

$$P_0 = (a \times P_s + b) \left(\frac{1}{\alpha A_e} \right) \left(\sqrt{\frac{2\pi k T_0}{m_a}} \right). \quad (6)$$

Using the highest and lowest coefficients presented in Table 1, it was possible to obtain the highest and lowest mass flow rate difference. Comparing this value with the average mass flow rate, it is possible to obtain the maximum and minimum percentage variation of 1.1% and 2.8%, respectively. As the plenum pressure variation does not cause such considerable changes in the mass flow rate, it was possible to combine the Eq. (1), with the analytical Eq. (2), and make practical use of the Eq. (6), varying the plenum pressure within the operating values described, with a maximum estimated margin of error of 2.8%.

Combining the analytical model for the thrust, Eq. (4), with the presented Eq. (6) for the plenum pressure variation as a function of the sublimation pressure inside the tank, we have

$$\mathfrak{S} = (a P_s + b) \frac{\pi + 2}{2\pi} \sqrt{T_w \frac{6\gamma}{\pi + 6\gamma} \frac{2\pi k}{m_a}} \quad (7)$$

which describes the thrust variation as a function of the sublimation pressure, meaning that the thruster performance can be controlled by the tank pressure and the wall temperature of the heater chip.

It is important to highlight that the proposed equations are valid for the boundary conditions presented by Guimarães and Guerrieri (2020). Summarizing the geometric conditions, a propellant tank as a soft thin tube with 0.8 mm diameter and a cylindrical plenum with 12 mm diameter were used to fit 1U of a CubeSat. Furthermore, and ambient temperature of 300 K was used in the simulations. The heater chip geometry considered in this paper was based on the work developed by Guerrieri *et al.* (2015). Therefore, the grid have different numbers of circular microchannels with 100 μm of diameter and 500 μm length. Additionally, the transmission coefficient was calculated using the Eq. (3) for the heater chip mentioned with $\delta = 5$, and the specific heat ratio was calculated based on water as a propellant.

4. RESULTS AND DISCUSSION

Figure 3 shows the plenum pressure variation as a sublimation pressure function, using Eq. (6). Which is a interesting relation, in order to control the plenum pressure by precisely controlling the sublimation pressure in the tank. The results demonstrate a pressure variation in the plenum and tank according to the expected operating conditions, with the plenum pressure varying between 81.4 and 171 Pa and the tank between 300 and 600 Pa. These results were based on a heater chip with 50 x 50 channels.

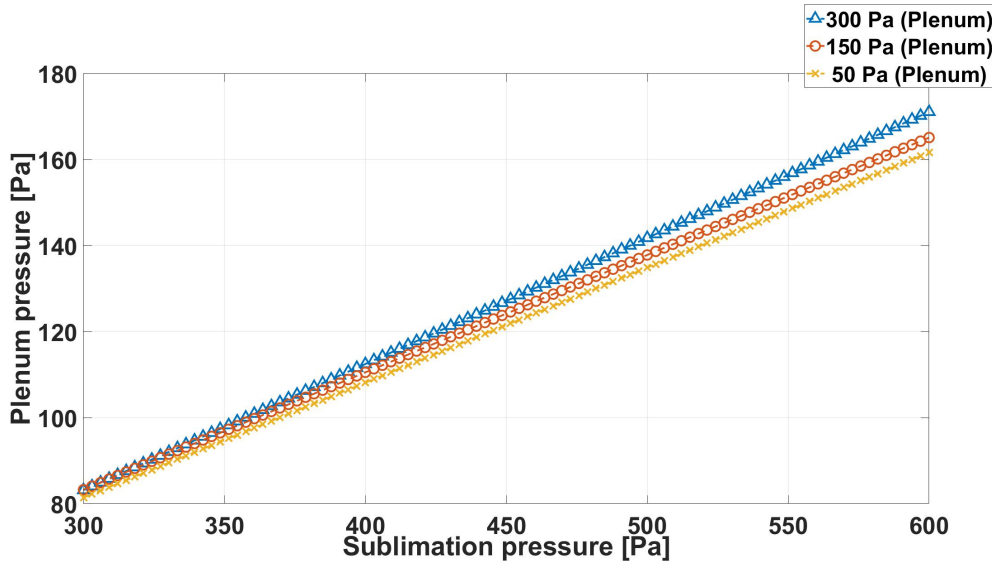


Figure 3. Sublimation pressure versus plenum pressure for a heater chip with 50 x 50 channels using the Eq. (6) with different coefficients from Table 1.

Another interesting parameter that can vary the plenum pressure is the channel geometry and number of channels present in the heater chip. As it can be observed in Eq. (6) the exit area takes into account the number of channels in the grid, by means, increasing the number of channels results in increasing the exit area and decreasing the plenum pressure. Similarly, changing the geometry from the circular channel to the squared slot, would result in an increase of almost two times the alpha value, causing a decrease in the plenum pressure.

Figure 4 shows the plenum and sublimation pressure variation for different numbers of channels in the heater chip. The previously mentioned operating pressure limits for the plenum and tank was established, in order to find the maximum and minimum viable number of channels for the described parameter constraints.

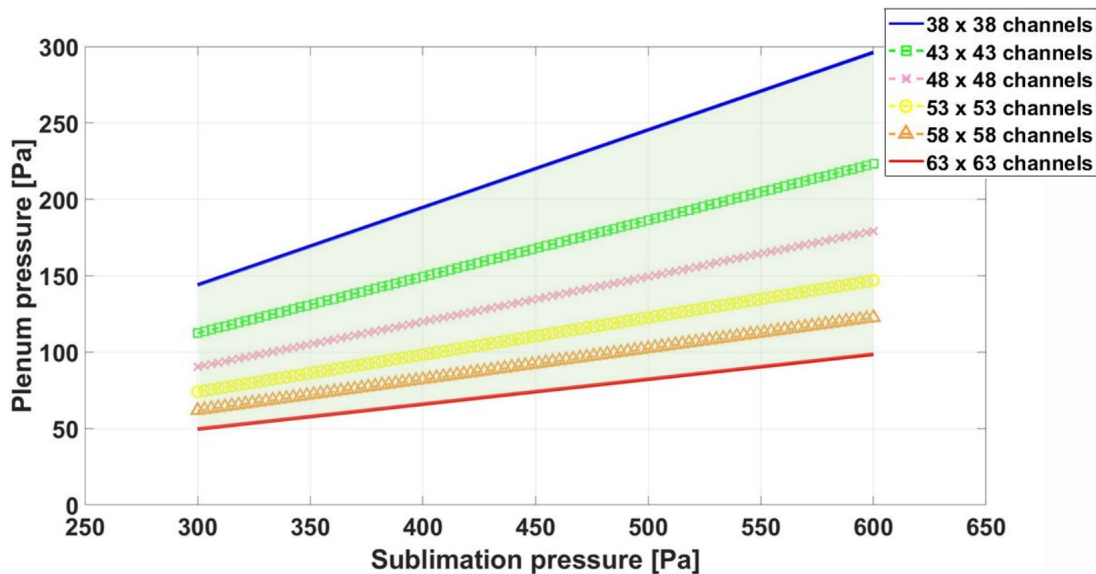


Figure 4. Different number of channels within the operational limit for the LPM

The highest operational limit was defined through the application of Eq. (6), using the the highest coefficients

in Table 1, with the maximum limit of 300 Pa possible for the plenum. The lowest operational limit was obtained similarly, using the the lowest coefficients in Table 1. With these limits established it was possible to find the maximum number of 63 x 63 channels and minimum number of 38 x 38 channels.

The hatched area in Figure 4 demonstrates the operational limit as a function of the number of viable channels, meaning that any number of channels chosen, under these conditions, will meet the imposed requirements. The intermediate cases from 43 x 43 to 58 x 58 channels were obtained through Eq. (6), using the coefficients for the medium case, with the plenum pressure of 150 Pa, in order to represent some of the possible scenarios.

In order to evaluate the thruster performance through the specific impulse and thrust results, varying the sublimation pressure inside the tank and the wall temperature of the heater chip. Equation (5) and (7) were used, see Table 2. The maximum thrust and specific impulse values are 0.77 mN and 117.55 s, respectively. These values occur when sublimation pressure and wall temperature are maximum, reaching 600 Pa and 900 K. The opposite relation is true for the minimum value of thrust and specific impulse of 0.22 mN and 67.87 s, respectively, which occurs for the minimum values of sublimation pressure and wall temperature, 300 Pa and 300 K, characterizing a directly proportional relationship between these quantities.

Table 2. Thruster performance comparison for different number of channels, wall temperature and plenum pressure

number of channels	P_s [Pa]	P_0 [Pa]	T_w [K]	\mathfrak{F} [mN]	I_{sp} [s]
38 × 38	300	144.1	300	0.22	67.87
38 × 38	450	214.94	300	0.33	67.87
38 × 38	600	285.79	300	0.44	67.87
38 × 38	300	144.1	900	0.39	117.55
38 × 38	450	214.94	900	0.58	117.55
38 × 38	600	285.79	900	0.77	117.55
63 × 63	300	52.43	300	0.22	67.87
63 × 63	450	78.2	300	0.33	67.87
63 × 63	600	103.98	300	0.44	67.87
63 × 63	300	52.43	900	0.39	117.55
63 × 63	450	78.2	900	0.58	117.55
63 × 63	600	103.98	900	0.77	117.55

Table 2 shows the thrust and specific values do not change as the exit area increases, but the plenum pressure does. Meaning that the same value for thrust and specific impulse can be obtained for different number of channels with different plenum pressure. This indicates that plenum pressure is a limiting factor to the system because it can not be lower than 50 Pa or higher than 300 Pa, avoiding flow regime variation and consequent thruster performance. In other words, once carefully decided the number of the channel of the heater chip, the thruster performance can be controlled by tank pressure and heater chip wall temperature. The performance range presented in Table 2 fits some mission requirements involving LPM, as described by Silva *et al.* (2018). Small satellites such as PocketQubes and CubeSats have lower power consumption and reduced mass, therefore, lower level of thrust can benefit them.

As previously mentioned, the results presenting the highest plenum pressure values are due to the grid with less number of channels, and the lowest pressure values occurred for grid with more number of channels. A key factor for the correct functioning of the LPM is the maintenance of high Knudsen number throughout the thruster part, ensuring a transitional regime for a better performance. Therefore, the estimations presented in this paper on the viable operational number of channels, can be used as a baseline for better sizing the ideal grid for the heater chip.

Other important parameters, such as the influence of temperature on the plenum, the channel geometry and the spacing between them were not investigated in this article. These topics can still be explored extensively in order to increase knowledge about the integration of all LPM parts.

5. CONCLUSION

In this paper, a hybrid analytical-numerical model was proposed to describe the interaction between sublimation pressure and plenum pressure, in order to estimate the performance of a LPM. This model aims to fill the gap between studies on the LPM propellant tank, integrating analytical models for the heater chip with numerical simulations involving the tank and the plenum. A set of new equations, with a maximum estimated error of 2,8%, were developed to evaluate the change of plenum pressure and thrust as a function of the sublimation pressure of the ice. The presented maximum and minimum values of thrust and specific impulse fit some LPM mission requirements.

One of the particularities of the LPM is its flexibility in terms of varying the number of channels in the heater chip grid. Therefore, it was investigated how the sublimation pressure influences the number of channels and the thrust performance according to the setted operational conditions. The next step would be to investigate the influence of other mentioned parameters, such as plenum temperature and different channel geometries.

6. ACKNOWLEDGMENT

This present work was supported by FAPERJ, Carlos Chagas Filho Foundation for Research Support of Rio de Janeiro State. The authors would also sincerely like to thank CEFET-RJ for supporting the development of this research.

7. REFERENCES

- Cervone, A., Mancas, A. and Zandbergen, B., 2015. "Conceptual design of a low-pressure micro-resistojet based on a sublimating solid propellant". *Acta Astronautica*, Vol. 108, pp. 30–39.
- Curzi, G., Modenini, D. and Tortora, P., 2020. "Large constellations of small satellites: A survey of near future challenges and missions". *Aerospace*, Vol. 7, No. 9, p. 133.
- Doncaster, B., Shulman, J., Bradford, J. and Olds, J., 2016. "Spaceworks' 2016 nano/microsatellite market forecast".
- Guerrieri, D.C., e Silva, M.d.A.C., Zandbergen, B. and Cervone, A., 2015. "Development of a low pressure free molecular micro-resistojet for cubesat applications". In *IAF 66th international astronomical congress, IAC2015, Jerusalem, Israel*. IAF, pp. 1–10.
- Guerrieri, D.C., Silva, M.A., Cervone, A. and Gill, E., 2017. "Selection and characterization of green propellants for micro-resistojets". *Journal of Heat Transfer*, Vol. 139, No. 10.
- Guerrieri, D.C., Silva, M.A., Cervone, A. and Gill, E., 2018a. "An analytical model for characterizing the thrust performance of a low-pressure micro-resistojet". *Acta Astronautica*, Vol. 152, pp. 719–726.
- Guerrieri, D.C., e Silva, M.d.A.C., Cervone, A. and Gill, E., 2018b. "Optimum design of low-pressure micro-resistojet applied to nano-and pico-satellites". In *ESA Space Propulsion 2018 Conference*. p. SP2018_00108.
- Guerrieri, D., Silva, M., Zandbergen, B. and Cervone, A., 2016. "Heater chip with different microchannels geometries for a low pressure free molecular micro-resistojet". *Space Propulsion 2016*.
- Guildner, L., Johnson, D. and Jones, F., 1976. "Vapor pressure of water at its triple point". *Journal of research of the National Bureau of Standards. Section A, Physics and chemistry*, Vol. 80, No. 3, p. 505.
- Guimarães, I. and Guerrieri, D., 2020. "Numerical analysis of the water vapour through the feed system of the low-pressure micro-resistojet". In *2020 18th Brazilian Congress of Thermal Sciences and Engineering (ENCIT)*. ABCM.
- Jensen, K.F. and Vinther, K., 2010. "Attitude determination and control system for aausat3". *Master's Thesis, Aalborg University*.
- Karniadakis, G., Beskok, A. and Aluru, N., 2006. *Microflows and nanoflows: fundamentals and simulation*, Vol. 29. Springer Science & Business Media.
- Malphrus, B.K., Freeman, A., Staehle, R., Klesh, A.T. and Walker, R., 2021. "Interplanetary cubesat missions". In *Cubesat Handbook*, Elsevier, pp. 85–121.
- Mitra, R.N. and Agrawal, D.P., 2015. "5g mobile technology: A survey". *ICT express*, Vol. 1, No. 3, pp. 132–137.
- O'Reilly, D., Herdrich, G. and Kavanagh, D.F., 2021. "Electric propulsion methods for small satellites: A review". *Aerospace*, Vol. 8, No. 1, p. 22.
- Pang, W., Bo, B., Meng, X., Yu, X., Guo, J. and Zhou, J., 2016. "Boom of the cubesat: A statistic survey of cubesats launch in 2003–2015". In *Proceedings of the 67th International Astronautical Congress (IAC), Guadalajara, Mexico*. pp. 26–30.
- Quinsac, G., Segret, B., Koppel, C. and Mosser, B., 2020. "Attitude control: A key factor during the design of low-thrust propulsion for cubesats". *Acta Astronautica*, Vol. 176, pp. 40–51.
- Silva, M.A., Guerrieri, D.C., Cervone, A. and Gill, E., 2018. "A review of mems micropropulsion technologies

for cubesats and pocketqubes”. *Acta Astronautica*, Vol. 143, pp. 234–243.

Xia, X., Sun, G., Zhang, K., Wu, S., Wang, T., Xia, L. and Liu, S., 2017. “Nanosats/cubesats adcs survey”. In *2017 29th Chinese Control And Decision Conference (CCDC)*. IEEE, pp. 5151–5158.